SCIENTIFIC REPORTS

OPEN

SUBJECT AREAS:
OPTICS AND PHOTONICS
OPTICAL MATERIALS AND STRUCTURES
NANOPARTICLES
APPLIED PHYSICS

Received
30 July 2012

Accepted
11 October 2012

Published
24 October 2012

Correspondence and requests for materials should be addressed to K.S. (sasaki@es.hokudai.ac.jp)

Nanoscale interference patterns of gap-mode multipolar plasmonic fields

Yoshito Tanaka, Akio Sanada & Keiji Sasaki

Research Institute for Electronic Science, Hokkaido University, Sapporo 001-0020, Japan.

Arbitrary spatial distributions of the electric field of light are formed through the interference of individual wavenumber mode fields with appropriate amplitudes and phases, while the maximum wavenumber in the far field is limited by the wavelength of light. In contrast, localized surface plasmons (LSPs) possess the ability to confine photons strongly into nanometer-scale areas, exceeding the diffraction limit. In particular, gap-mode LSPs produce single-nanometer-sized, highly intense localized fields, known as hot spots. Here, we show the nanoscale spatial profiles of the LSP fields within hot spots, which exhibit complicated fine structures, rather than single peaks. The nanopatterns are created by constructive and destructive interferences of dipolar, quadrupolar, and higher-order multipolar plasmonic modes, which can be drastically altered by controlling parameters of the excitation optical system. The analysis in this study would be useful for proposing new concepts for manipulation and control of light-matter interactions in nanospaces.

Nanoscale spatial confinement of the electric field can be achieved by LSP polaritons of metal nanostructures[1–4], which strongly enhances photophysical and photochemical processes[5–9]. One promising structure is a dimer of metal nanoparticles with a nanometer-sized separation, which can produce an intense electric field within the nanogap[10–15], called the hot spot. The extreme field enhancement and localization effects are caused by strong interaction between the plasmonic resonances of the two particles. The hot spot provides an enormous spatial gradient of the electric field[16], which induces a strong radiation pressure exerted even on a single molecule[17,18]. When the spot size is comparable to the spread of the molecular electric wavefunctions, anomalous excited-state dynamics[19] that break the long wavelength approximation appears. Furthermore, the small mode volume provided by the gap-mode LSP enhances exciton-photon coupling, allowing vacuum Rabi splitting to be successfully observed[20–22]. These applications of the hot spot could be advanced if the spatial pattern of the gap-mode LSP field could be externally controlled.

Here, we consider metal nanodisks for simplicity. When an incident electric field couples with coherent electron oscillations in a metal disk, surface charge density waves propagate circularly around the disk's edge. The resonance condition for the round-trip propagation determines the angular modes, which are numbered by integers n and are known as the whispering gallery modes. The lowest-order mode ($n=1$), i.e., the dipolar resonance, can be excited by illumination with circularly polarized light. For linearly polarized light, i.e., superpositions of right- and left-handed circular polarizations, counter-propagating waves interfere with each other to produce a standing wave around the disk. The second-order mode ($n=2$), i.e., the quadrupolar resonance, cannot couple to plane-wave light at normal incidence.

When two nanodisks are placed in close proximity, the charge density waves propagating in the individual disks interact strongly with each other. The attractive Coulomb interaction in the nanogap region slows the plasmonic wave, thereby redshifting the resonant frequency and increasing the charge density and the field intensity around the nanogap (see Supplementary Videos S1 and S2). Because this interaction breaks the symmetry of the charge distribution, the quadrupolar mode becomes able to couple to normally incident plane-wave light. When multiple angular modes are simultaneously excited, they interfere with each other, which results in Fano-like resonances appearing in the far-field scattering spectra[23]. In particular, the destructive interference can be used to achieve efficient photon harvesting from the far field to the nanospace without the scattering loss. In this study, we investigated the constructive and destructive interference of the gap-mode multipolar plasmonic resonances in the near-field range, which manifest as dramatic variation of the electric field distributions within the hot spot.

Results

Model system with multipolar plasmonic resonances. We performed numerical simulations of the gap-mode LSP field. Figure 1a shows a schematic of the model system, which consists of two gold disks separated by a

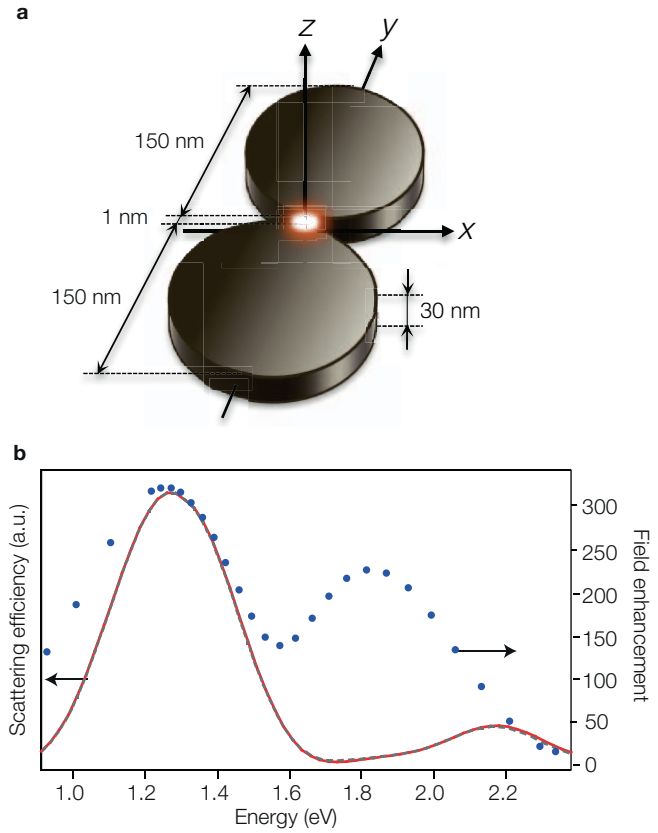

Figure 1 | Structural geometry of a metal nanodisk dimer and its spectral responses. (a) A schematic of a model system consisting of two gold disks separated by a nanogap. The surrounding medium is air. The origin of the three-dimensional Cartesian coordinate system is positioned at the center of the disk dimer structure; the *y*-axis is along the dimer axis, and the *x*- and *z*-axes are set to be parallel and perpendicular to the flat surfaces of the disks, respectively. (b) Scattering spectra of the gold disk dimer illuminated at normal incidence (red) and at oblique (45°) incidence (gray broken). The blue dots show an enhancement spectrum of the LSP field at the center of the gap, where the field enhancement is defined as the absolute amplitude normalized by the incident field, $|E_y/E_0|$.

nanogap. The system is similar to structures that were fabricated and analyzed in our previous work[12]. Recently, the resolution of the fabrication technique for gold nanogap is pushed to <1-nm level using an electron-beam lithography processes[24–26]. The disk dimer is excited by normal illumination of plane-wave light linearly polarized along the dimer axis (the *y*-direction in Fig. 1a). The far-field scattering spectrum (red curve in Fig. 1b) exhibits the dipolar plasmonic resonance as the lowest frequency peak at 1.29 eV, and the small resonance peak at 2.14 eV corresponds to the quadrupolar mode. Note that the dipolar mode of a single nanodisk exhibits a resonant peak at 2.06 eV, and the surface plasmon frequency of gold is 2.5 eV.

Excitation frequency dependence of gap-mode LSP fields. Figure 2 shows steady-state spatial distributions of the gap-mode LSP fields. At the incident light frequency of 1.29 eV (Fig. 2a), where the dipolar resonance is excited, the gap-mode LSP field along the *x*-axis exhibits a single-peak profile with a width of 14.0 nm. When the excitation frequency is increased to 1.82 eV (Fig. 2b), the peak shape narrows (9.8-nm width) and forms small sidelobes with a phase of $-\pi$ relative to the main peak. At this frequency, the dipolar and quadrupolar modes are both excited, and radiations from those resonances destructively interfere such that the far-field scattering is suppressed. In the near-field range, the gap-mode LSP fields of the dipolar and quadrupolar resonances induce constructive interference at the center of the peak and destructive interference at the shoulders ($x \sim \pm 10$ nm), producing the observed intense narrow peak shape. The field enhancement spectrum at the center of the gap (blue dots in Fig. 1b) exhibits a secondary-large peak at 1.82 eV. This result is similar to that of the reported work by McMahon *et al.*[27], which showed that the field enhancement spectrum is the lack of correlation with the far-field optical spectrum. At the excitation frequency of 2.14 eV (Fig. 2c), the quadrupolar mode profile dominates, and the dipolar mode shape is superposed. When the excitation frequency is further increased, destructive interference of the mode fields at the center of the gap gives rise to anomalous shapes, such as three distinct peaks separated by 10-nm intervals (Fig. 2d) or a central dip profile (Fig. 2e).

Because all LSP field distributions can be expressed as linear combinations of the individual angular mode profiles, we performed eigenanalysis of the real and imaginary parts of the five spatial profiles presented in Fig. 2. The sum of the two largest eigenvalues is 99.3% of the total value, and the sum of the three largest is 99.9%. The corresponding eigenfunctions are unitarily transformed to three orthogonal bases such that the first basis (Fig. 3a) is a curve optimally fitted to the dipolar mode profile presented in Fig. 2a. The second and third basis functions (Fig. 3b,c) correspond closely to the spatial mode profiles of the quadrupolar and hexapolar plasmonic resonances, respectively. These curves demonstrate that the spatial periods of the charge density waves are strongly compressed in the gap region due to the slowed plasmonic wave propagation. The left diagrams in Fig. 3a–c show schematics of the charge distributions of the individual angular modes. Note that the distributions of these three modes are symmetric with respect to the *y*-axis, and the signs of the charges alternate following the oscillation of the incident field. Because the dipolar charge oscillation is delayed by a phase of nearly π from the quadrupolar oscillation at the incident frequency of 1.82 eV, the field profile (Fig. 2b) is approximately given by subtracting these two mode profiles (Fig. 3,b), which gives rise to the intense and narrow peak.

Interference patterns of gap-mode LSP fields with oblique illumination system. The individual angular modes are doubly degenerate, which corresponds to counter-propagating wave modes. These modes can be unitarily transformed into two orthogonal standing wave modes that have symmetric and antisymmetric charge distributions with respect to the *y*-axis. The symmetric distribution mode can be excited by normally incident plane-wave light, as described above, while the antisymmetric mode cannot. Here, we employ an oblique illumination system to excite the antisymmetric distribution mode. Figures 4a–c display the spatial distributions of the gap-mode LSP fields excited by a *y*-directionally *s*-polarized plane-wave at an incidence angle of 45°. The scattering spectrum under oblique illumination (gray broken curve in Fig. 1b) exhibits no appreciable difference from that produced under normal illumination. Additionally, the LSP field profile obtained at the dipolar resonance frequency (Fig. 4a) is shaped nearly the same as it is under normal illumination (Fig. 2a). In contrast, the amplitude and phase profiles at the excitation frequencies 1.82 and 2.14 eV (Fig. 4b,c) are asymmetric and include π-phase jumps. We also analyzed these spatial profiles to determine the eigenfunctions, and the calculation shows that the profiles can be reconstructed from the two basis functions presented in Fig. 3a,b and the additional basis function shown in Fig. 3d. This curve corresponds to the field profile of the quadrupolar antisymmetric distribution mode, whose charge distribution is illustrated in the left diagram of the figure.

We also investigated a sophisticated illumination system in which two coherent plane-waves are incident on the dimer structure at angles of $\pm 45°$. The excitation light frequency is fixed to the quadrupolar resonant peak at 2.14 eV. When the two plane-waves are

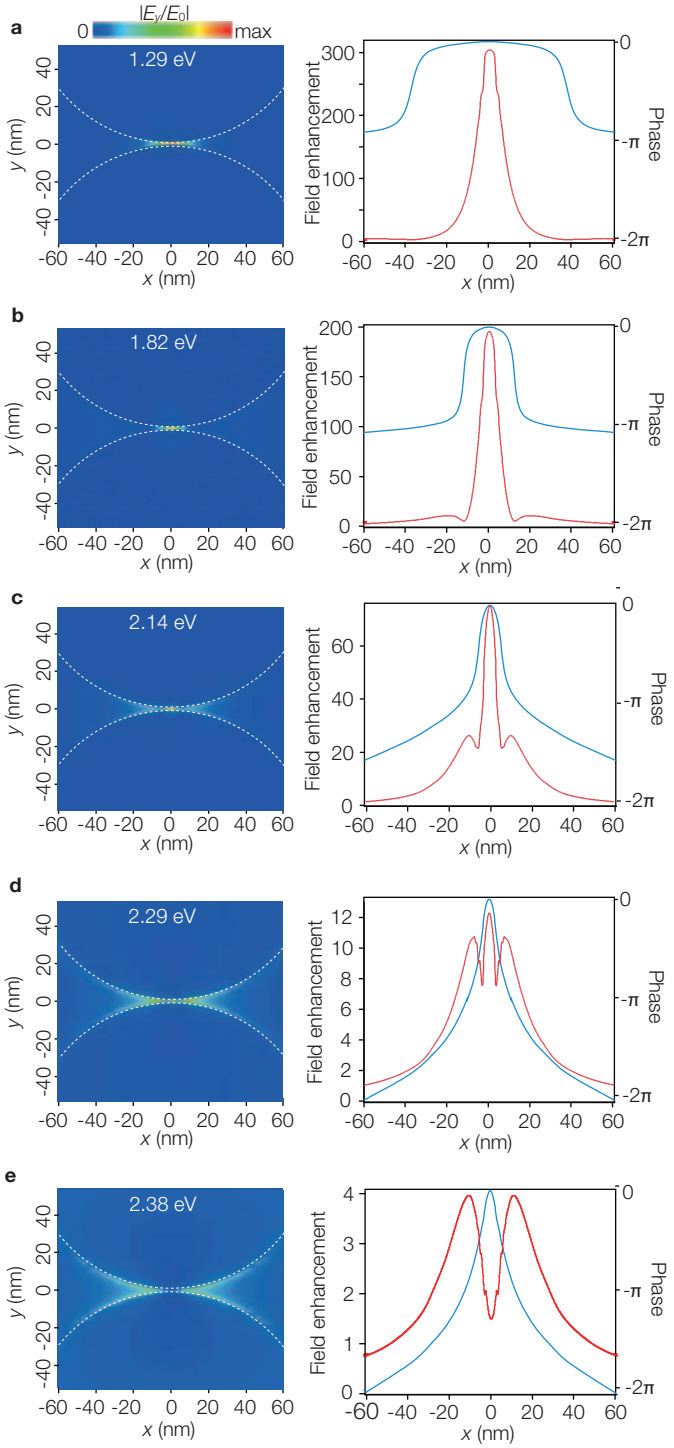

Figure 2 | Spatial distributions of the LSP fields formed by normal illumination at different excitation frequencies. The left patterns display the *y*-component of the electric field E_y on the *x*-*y*-plane at $z=0$, where the absolute amplitude $|E_y|$ normalized by the maximum value in each pattern is presented using color. The right figures show the cross-sectional profiles of the field amplitude (red) and phase (blue) within the gap along the *x*-axis at $y=z=0$. The amplitude is plotted on a field-enhancement scale, and the phase is relative to that at the center ($x=0$).

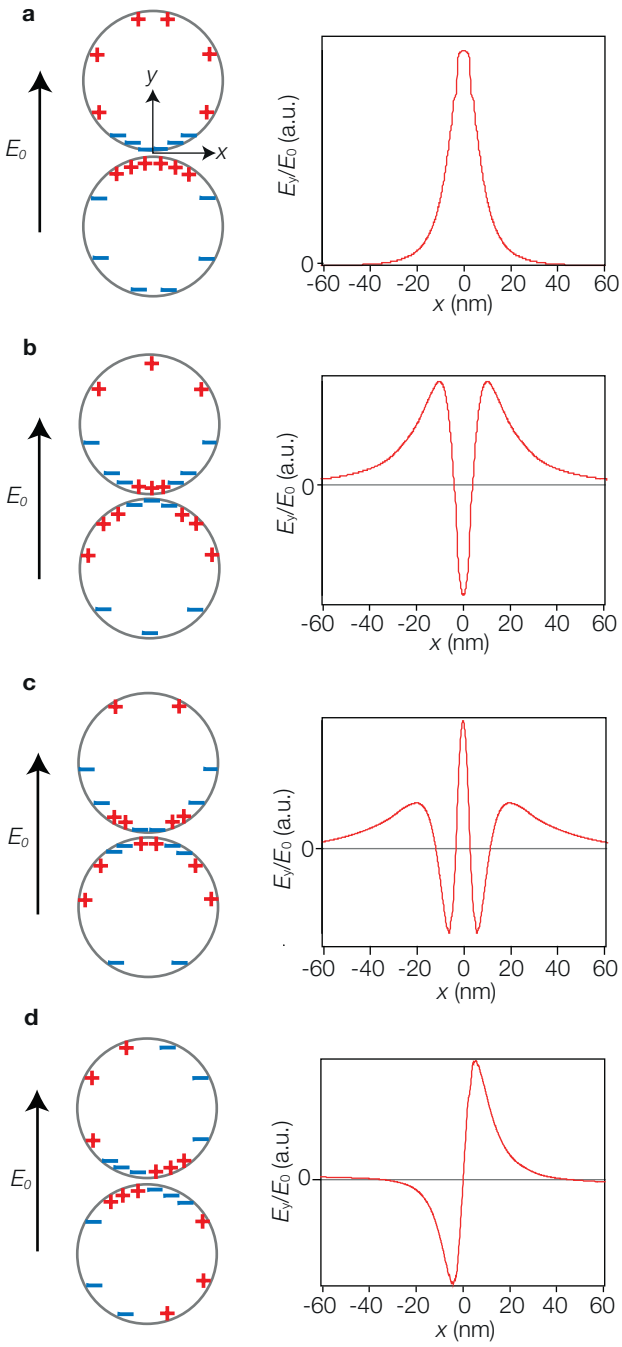

Figure 3 | Charge distributions and field profiles of individual multipolar plasmonic modes. (a)–(c), Orthogonal basis functions calculated by eigenanalysis of the real and imaginary parts of the cross-sectional profiles in Fig. 2 (right) and schematic illustrations of the charge distributions of the individual angular mode resonances (left). The three functions correspond closely to the spatial mode profiles of the dipolar (a), quadrupolar (b), and hexapolar (c) plasmonic fields. (d) An additional basis function determined by eigenanalysis of the profiles shown in Fig. 4a–c (right) and a schematic of the corresponding charge distribution (left). The curve is the third eigenfunction, and the first and second basis functions are much the same as the orthogonal functions presented in (a) and (b). This profile corresponds closely to the antisymmetric distribution mode of the quadrupolar resonance.

in-phase at the origin (Fig. 4d), a symmetric field profile similar to the profile shown in Fig. 2c (normal incidence) appears. When the phase difference is increased to π/2 (Fig. 4e), the spatial profile becomes asymmetric and similar to that presented in Fig. 4c (oblique incidence). By introducing two plane-waves with inverted phases (Fig. 4f), all symmetric distribution modes are cancelled by destructive interference, and the quadrupolar antisymmetric distribution mode is excited within the gap. This profile exhibits a narrow dip (2.6-nm width) and a phase jump of π at the center.

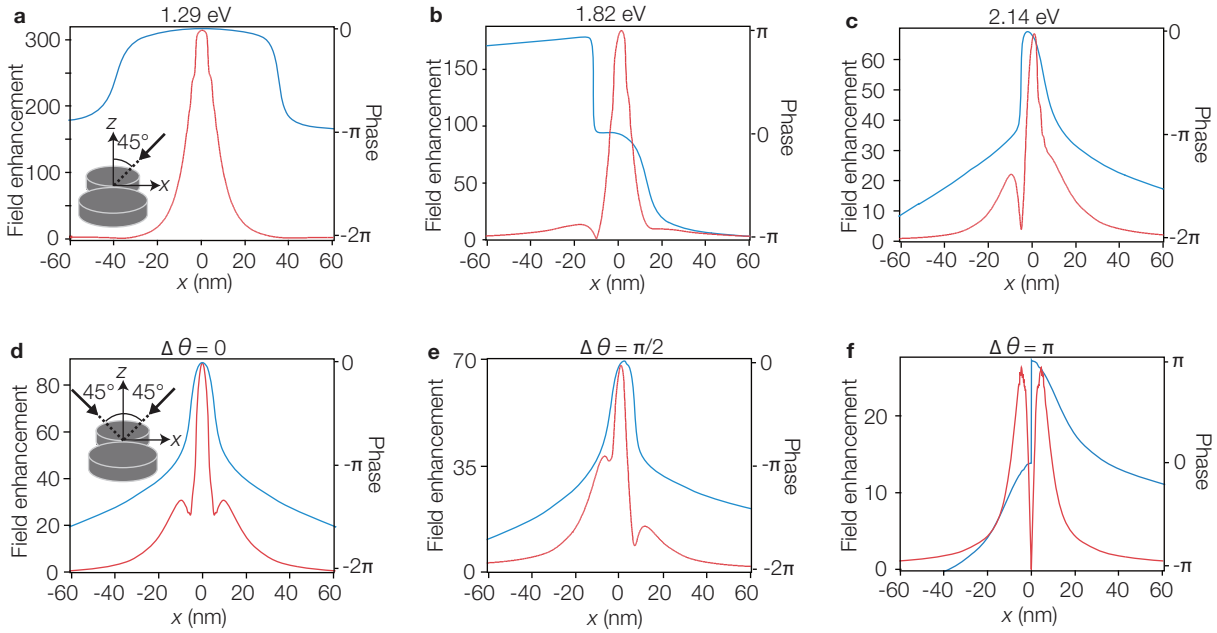

Figure 4 | Cross-sectional profiles of the LSP fields formed by oblique illumination. Amplitude (red) and phase (blue) profiles of the electric field E_y within the gap are plotted against the *x*-axis. (a)–(c), The dimer structure is illuminated with a *y*-directionally *s*-polarized plane-wave at an incidence angle of 45°. The LSP fields are excited at three different frequencies. (d)–(f), The LSP fields are formed by dual-plane-wave oblique illumination with two *y*-directionally *s*-polarized lights incident at angles of ±45° (normal intersection). The phase difference between the two plane-waves is set to 0 (d), π/2 (e), and π (f).

Discussion

To conclude, the nanoscale spatial distributions of gap-mode LSP fields in a gold nanodisk dimer system have been analyzed. A variety of finely structured profiles are formed by constructive and destructive interference of symmetric and antisymmetric multipolar plasmonic mode fields, which can be controlled through the excitation frequency and configuration of the illumination system. Many other adjustable parameters are available, including the sizes, shapes, gap distances, and materials of the metal nanoparticles, as well as the incident angles, wavefront shapes, and polarizations of the illumination optics. Further quantitative analysis of the LSP fields could be performed by including quantum mechanical[28,29] and nonlocal effects[30], which are indispensable for the case of the dimer separation below 1 nm. Realization of nanoscale field manipulation would prove crucial to studies of the light-matter interactions in plasmonic nanospaces as well as to the development of future nanophotonic devices. The enormous spatial gradient of the electric field induces a strong radiation pressure for nanometer-sized objects such as quantum dots, molecular assemblies, and metal cluster compounds. Control of nanoscale electric fields proposed in our study can be expected to realize stable optical trapping and flexible manipulation of the nanosized objects. In addition, interactions between the finely structured LSP fields and molecular electric wavefunctions can dramatically modulate the optical selection rules for dark and bright excited-states of molecules and nanomaterials.

Methods

We numerically analyzed the gap-mode LSP fields using a three-dimensional finite-difference time domain algorithm. In contrast to mathematical methods based on transformation optics[23] that analytically solve the dimer system, this simulation method has the flexibility to model nanostructures and illumination systems. The frequency dispersion of the complex permittivity of gold measured by Johnson and Christy[31] was utilized. In the numerical simulation, the three-dimensional space was discretized using the nonuniform mesh method with a unit cell size of 0.1 x 0.1 x 0.1 nm^3 within the gap, which is the resolution necessary for accurate analysis. The number of iterations was set to 10^5 steps to ensure complete convergence. The scattering spectra of the gold disk dimer under normal and oblique illumination were obtained by Fourier transformation of the temporal responses to short pulse excitations.

1. Maier, S. A. *et al.* Local detection of electromagnetic energy transport below the diffraction limit in metal nanoparticle plasmon waveguides. *Nature Mat* **2**, 229–232 (2003).
2. Feng, L. *et al.* Nanoscale optical field localization by resonantly focused plasmons. *Opt. Express* **17,** 4824–4832 (2009).
3. Jon A. Schuller *et al.* Plasmonics for extreme light concentration and manipulation. *Nature Mat* **9,** 193–204 (2010).
4. Brongersma, M. L. & Kik, P. G. *Surface Plasmon Nanophotonics* (Springer, Dordrecht, 2007).
5. Moskovits, M. Surface-enhanced spectroscopy. *Rev. Mod. Phys.* **57**, 783–826 (1985).
6. Nie, S. & Emory, S. R. Probing single molecules and single nanoparticles by surface-enhanced Raman scattering. *Science* **275**, 1102–1106 (1997).
7. Kneipp, K. *et al.* Single molecule detection using surface-enhanced raman scattering (SERS). *Phys. Rev. Lett.* **78**, 1667–1670 (1997).
8. Kinkhabwala, A. *et al.* Large single-molecule fluorescence enhancements produced by a bowtie nanoantenna. *Nature Photon* **3**, 654–657 (2009).
9. Ueno, K. *et al.* Nanoparticle plasmonassisted two-photon photolymerization induced by incoherent excitation source. *J. Am. Chem. Soc.* **130**, 6928–6929 (2008).
10. Xu, H., Aizpurua, J., Käll, M. & Apell, P. Electromagnetic contributions to single-molecule sensitivity in surface-enhanced Raman scattering. *Phys. Rev. E* **62**, 4318–4324 (2000).
11. Hao, E. & Schatz, G. C. Electromagnetic fields around silver nanoparticles and dimers. *J. Chem. Phys.* **120**, 357–366 (2004).
12. Tanaka, Y. *et al.* Direct imaging of nanogap-mode plasmon-resonant fields. *Opt. Express* **19**, 7726–7733 (2011).
13. Mühlschlegel, P., Eisler, H.-J., Martin, O. J. F. & Hecht, B. Resonant optical antenna. *Science* **308**, 1607–1609 (2005).
14. Fischer, H. & Martin, O. J. F. Engineering the optical response of plasmonic nanoantennas. *Opt. Express* **16**, 9144–9154 (2008).
15. Imura, K., Okamoto, H., Hossain, M.-K. & Kitajima, M. Visualization of localized intense optical fields in single gold-nanoparticle assemblies and ultrasensitive raman active sites. *Nano. Lett.* **6**, 2173–2176 (2006).
16. Zhang, W., Huang, L., Santschi, C. & Martin, O. J. F. Trapping and sensing 10 nm metal nanoparticles using plasmonic dipole antennas. *Nano Lett* **10**, 1006–1011 (2010).
17. Xu, H. & Kall, M. Surface-plasmon-enhanced optical forces in silver nanoaggregates. *Phys. Rev. Lett.* **89**, 246802 (2002).
18. Tanaka, Y., Yoshikawa, H., Itoh, T. & Ishikawa, M. Surface enhanced raman scattering from pseudoisocyanine on Ag nanoaggregates produced by optical trapping with linearly polarized laser beam. *J. Phys. Chem. C* **113**, 11856–11860 (2009).
19. Iida, T., Aiba, Y. & Ishihara, H. Anomalous optical selection rule of an organic molecule controlled by extremely localized light field. *Appl. Phys. Lett.* **98**, 053108 (2011).

20. Wu, X., Gray, S. K. & Pelton, M. Quantum-dot-induced transparency in a nanoscale plasmonic resonator. *Opt. Express* **18**, 23633–23645 (2010).
21. Savasta, S. *et al*. Nanopolaritons: vacuum rabi splitting with a single quantum dot in the center of a dimer nanoantenna. *ACS NANO* **4**, 6369–6376 (2010).
22. Manjavacas, A., Abajo, F. J. García De & Nordlander, P. Quantum plexcitonics: strongly interacting plasmons and excitons. *Nano Lett.* **11**, 2318–2323 (2011).
23. Aubry, A., Lei, D. Y., Maier, S. A. & Pendry, J. B. Interaction between plasmonic nanoparticles revisited with transformation optics. *Phys. Rev. Lett.* **105**, 233901 (2010).
24. Ueno, K., Juodkazis, S., Mizeikis, V., Sasaki, K. & Misawa, H. Clusters of closely-spaced gold nanoparticles as a source of two-photon photoluminescence at visible wavelengths. *Adv. Mater.* **20**, 26–30 (2008).
25. Berthelot, J. *et al*. Silencing and enhancement of second-harmonic generation in optical gap antennas. *Opt. Express* **20**, 10498–10508 (2012).
26. Duan, H., Fernandez-Dominguez, A. I., Bosman, M., Maier, S. A. & Yang, J. K. W Nanoplasmonics: Classical down to the Nanometer Scale. *Nano Lett.* **12**, 1683–1689 (2012).
27. McMahon, J. M., Li, S., Ausman, L. K. & Schatz, G. C. Modeling the effect of small gaps in surface-enhanced Raman spectroscopy. *J. Phys. Chem. C* **116**, 1627–1637 (2012).
28. Zuloaga, J., Prodan, E. & Nordlander, P. Quantum description of the plasmon resonances of a nanoparticle dimer. *Nano Lett.* **9**, 887–891 (2009).
29. Esteban, R., Borisov, A. G., Nordlander, P. & Aizpurua J. Bridging quantum and classical plasmonics with a quantum-corrected model. *Nature Comm* **3**, 825 (2012).
30. McMahon, J. M., Gray, S. K. & Schatz, G. C. Optical properties of nanowire dimers with a spatially nonlocal dielectric function. *Nano Lett* **10**, 3473–3481 (2010).
31. Johnson, P. B. & Christy, R. W. Optical constants of nobel metals. *Phys. Rev. B* **6**, 4370–4379 (1972).

Acknowlegements

The authors would like to thank T. Okamoto (Riken) and T. Itoh (AIST) for discussions and comments. This work was supported by a Grant-in-Aid for Scientific Research (A) and Young Scientists (B) from the Ministry of Education, Culture, Sports, Science, and Technology of Japan.

Author contributions

Y.T. and A.S. performed the numerical simulations. All authors discussed the results. Y.T. and K.S. wrote the manuscript, and K.S. supervised the research work.

Additional information

Supplementary information accompanies this paper at http://www.nature.com/scientificreports

Competing financial interests: The authors declare no competing financial interests.

How to cite this article: Tanaka, Y., Sanada, A. & Sasaki, K. Nanoscale interference patterns of gap-mode multipolar plasmonic fields. *Sci. Rep.* **2**, 764; DOI:10.1038/srep00764 (2012).